On the design of flux limiters for finite element discretizations with a consistent mass matrix

D. Kuzmin*

Institute of Applied Mathematics (LS III), University of Dortmund
Vogelpothsweg 87, D-44227, Dortmund, Germany

Abstract

The *algebraic flux correction* (AFC) paradigm is extended to finite element discretizations with a consistent mass matrix. A nonoscillatory low-order scheme is constructed by resorting to mass lumping and conservative elimination of negative off-diagonal coefficients from the discrete transport operator. In order to recover the high accuracy of the original Galerkin scheme, a limited amount of compensating antidiffusion is added in regions where the solution is sufficiently smooth. The raw antidiffusive fluxes, which include a contribution of the consistent mass matrix, are limited node-by-node so as to satisfy algebraic constraints imposed on the discrete solution. The proposed limiting strategy combines the advantages of multidimensional FEM-FCT and FEM-TVD schemes introduced previously. Its performance is illustrated by application to scalar convection problems in 1D and 2D.

Key Words: convection-dominated problems; high-resolution schemes; flux correction; finite elements; consistent mass matrix

1 Introduction

The advent of *flux-corrected transport* (FCT) and *total variation diminishing* (TVD) methods paved the way to the development of nonlinear high-resolution schemes based on flux/slope limiters. However, a serious disadvantage of many limiting techniques available to date is the lack of generality which precludes their use in the finite element framework. In a series of recent publications [13],[14],[15],[16], we developed an algebraic approach to the design of *local extremum diminishing* (LED) schemes by adding discrete (anti-)diffusion so as to enforce the M-matrix property in a conservative fashion. The underlying Galerkin discretization of high order was equipped with the (symmetric) FCT limiter or its (upwind-biased) counterparts of TVD type. In either case, the antidiffusive fluxes were limited **node-by-node** as proposed by Zalesak [28]. Promising results were obtained for scalar conservation laws as well as for the compressible Euler and incompressible Navier-Stokes equations on unstructured grids [16],[17],[25].

Algebraic flux correction of FCT type is applicable to Galerkin schemes with a consistent mass matrix and yields highly accurate solutions to time-dependent problems. However, it is not to be recommended for steady-state computations due to the fact that the correction factors depend on the time step. On the other hand, TVD-like schemes

*Correspondence to: kuzmin@math.uni-dortmund.de

lend themselves to the treatment of stationary problems but mass lumping is mandatory and there is an alarming ambiguity in the choice of the limiter function. In the present paper, we get rid of this ambiguity by constraining the *target flux* [29] which corresponds to the original Galerkin discretization. Building on our experience with algebraic FCT and TVD schemes, we design a symmetric limiter for the contribution of the consistent mass matrix and blend it with an upwind-biased limiter for the discretized convective term. As a result, we obtain a high-resolution finite element scheme which yields time-accurate solutions to transient problems and, moreover, does not suffer from a loss of accuracy if large time steps are employed when the solution approaches a highly convective steady state. Numerical examples are presented for 1D and 2D benchmark problems.

2 Linear high-order scheme

As a model problem, consider the time-dependent continuity equation

$$\frac{\partial u}{\partial t} + \nabla \cdot (\mathbf{v}u) = 0 \tag{1}$$

discretized in space by a high-order finite element method which yields an ODE system for the vector of time-dependent nodal values

$$M_C \frac{\mathrm{d}u}{\mathrm{d}t} = Ku, \tag{2}$$

where $M_C = \{m_{ij}\}$ denotes the consistent mass matrix and $K = \{k_{ij}\}$ is the discrete transport operator. A common practice in the FEM community is to employ the *group finite element formulation* as proposed by Fletcher [9]

$$u_h = \sum_j u_j \varphi_j, \qquad (\mathbf{v}u)_h = \sum_j (\mathbf{v}_j u_j)\, \varphi_j, \tag{3}$$

where φ_j refers to the basis function for node j. The use of these approximations in the weak form of (1) leads to the following formulae for the computation of matrix entries

$$m_{ij} = \int_\Omega \varphi_i \varphi_j \,\mathrm{d}\mathbf{x}, \qquad k_{ij} = -\mathbf{v}_j \cdot \mathbf{c}_{ij}, \qquad \mathbf{c}_{ij} = \int_\Omega \varphi_i \nabla \varphi_j \,\mathrm{d}\mathbf{x}. \tag{4}$$

The operator K may also contain some streamline diffusion used for stabilization purposes and/or to achieve better phase accuracy in the framework of Taylor-Galerkin methods [5]. This sparse matrix can be decomposed into the skew-symmetric part $K' := \frac{1}{2}(K - K^T)$ and the symmetric part $S := K - K'$ such that

$$k'_{ij} = \frac{k_{ij} - k_{ji}}{2} = -k'_{ji}, \qquad s_{ij} = \frac{k_{ij} + k_{ji}}{2} = s_{ji}. \tag{5}$$

Integration by parts reveals that the discrete gradient operator is skew-symmetric, i.e., $\mathbf{c}_{ij} = -\mathbf{c}_{ji}$. Therefore, the coefficients defined by (4)-(5) correspond to

$$k'_{ij} = -\frac{\mathbf{v}_i + \mathbf{v}_j}{2} \cdot \mathbf{c}_{ij}, \qquad s_{ij} = \frac{\mathbf{v}_i - \mathbf{v}_j}{2} \cdot \mathbf{c}_{ij}. \tag{6}$$

The contribution of streamline diffusion (if any) belongs into the symmetric part s_{ij}.

As explained in [26],[27], a skew-symmetric discretization is consistent with the properties of the continuous convective derivative $\mathbf{v}\cdot\nabla$ and implies the conservation of kinetic energy in turbulent flow computations. Any symmetric contribution S results in a non-physical but sometimes desirable production or dissipation of kinetic energy. Symmetric matrices with zero row/column sums can be classified as discrete diffusion/antidiffusion operators [13]. As we are about to see, they constitute a handy tool for the design of multidimensional high-resolution schemes on unstructured meshes.

3 Linear low-order scheme

For the numerical scheme to be nonoscillatory, it should possess certain properties, e.g., be monotone, total variation / local extremum diminishing, positivity- or monotonicity-preserving and/or satisfy the discrete maximum principle. These well-known criteria can be expressed as algebraic constraints to be imposed on a linear high-order discretization such as (2). For instance, if each solution update $u^n \rightarrow u^{n+1}$ or the converged steady-state solution $u^{n+1} = u^n$ satisfy a (nonlinear) algebraic system of the form

$$Au^{n+1} = Bu^n, \tag{7}$$

where $A = \{a_{ij}\}$ is an M-matrix and $B = \{b_{ij}\}$ has no negative entries, then the positivity of the old solution carries over to the new one [14],[16]

$$u^n \geq 0 \qquad \Rightarrow \qquad u^{n+1} = A^{-1}Bu^n \geq 0. \tag{8}$$

In the linear case, the M-matrix property can be readily enforced by resorting to 'discrete upwinding' [14],[15],[16]. In essence, the consistent mass matrix M_C is replaced by its lumped counterpart $M_L = \mathrm{diag}\{m_i\}$ and the high-order operator K is rendered local extremum diminishing by adding an artificial diffusion operator D designed so as to eliminate all negative off-diagonal coefficients. These straightforward algebraic manipulations yield a nonoscillatory low-order scheme of the form

$$M_L \frac{\mathrm{d}u}{\mathrm{d}t} = Lu, \qquad \text{where} \quad Lu = Ku + Du. \tag{9}$$

By construction, the diffusive term Du can be decomposed into a sum of skew-symmetric internodal fluxes associated with the edges of the sparsity graph [16]

$$(Du)_i := -\sum_{j\neq i} f_{ij}, \qquad \text{where} \quad f_{ij} = d_{ij}(u_i - u_j) = -f_{ji}. \tag{10}$$

The artificial diffusion coefficient d_{ij} for the edge $\overrightarrow{ij}$ is defined as follows

$$d_{ij} = d'_{ij} - s_{ij}, \qquad \text{where} \quad d'_{ij} = |k'_{ij}|. \tag{11}$$

Thus, the off-diagonal coefficients of the low-order operator are given by

$$l_{ij} := k_{ij} + d_{ij} = k'_{ij} + |k'_{ij}|. \tag{12}$$

Without loss of generality, the edge $\overrightarrow{ij}$ is oriented so that $k'_{ij} < 0$, which results in $l_{ij} = 0$ and $l_{ji} = 2d'_{ij}$. This convention implies that node i is located 'upwind' and corresponds to the row number of the eliminated negative coefficient [15],[16].

The semi-discretized equation for the nodal value u_i can be represented as

$$m_i \frac{\mathrm{d}u_i}{\mathrm{d}t} = \sum_{j \neq i} l_{ij}(u_j - u_i) + u_i \sum_j k_{ij}, \tag{13}$$

where $m_i = \sum_j m_{ij} > 0$ and $l_{ij} \geq 0$, $\forall i \neq j$. The last term in the above expression vanishes for discretely divergence-free velocity fields and is responsible for a physical growth of local extrema otherwise [16]. It can readily be seen that (cf. [11])

$$u_i(t) = 0, \quad u_j(t) \geq 0, \quad \forall j \neq i \qquad \Rightarrow \qquad \frac{\mathrm{d}u_i}{\mathrm{d}t} \geq 0, \tag{14}$$

which proves that the low-order scheme (9) is positivity-preserving. For its fully discrete counterpart to inherit this property, the time step should satisfy a CFL-like condition that ensures the positivity of diagonal coefficients in the right-hand side of (7).

4 Nonlinear high-resolution scheme

The high-resolution finite element schemes to be derived in this paper represent a nonlinear combination of the high-order Galerkin scheme (2) and its overly diffusive low-order counterpart (9). After the discretization in time by the standard θ-scheme, the algebraic systems for these linear methods are related by the formula [13]

$$[M_L - \theta \Delta t L]u^{n+1} = [M_L + (1-\theta)\Delta t L]u^n + \Delta t F(u^{n+1}, u^n). \tag{15}$$

The contribution of the last term to each node has the following structure

$$F_i(u^{n+1}, u^n) = \sum_{j \neq i} f_{ij}, \tag{16}$$

where f_{ij} denotes the *raw antidiffusive flux* (from node j into node i) which offsets the error induced by mass lumping and discrete upwinding:

$$f_{ij} = m_{ij}(\dot{u}_i - \dot{u}_j) + d_{ij}(u_i - u_j) = -f_{ji}. \tag{17}$$

Here and below

$$\dot{u}_i = \frac{u_i^{n+1} - u_i^n}{\Delta t}, \qquad u_i = \theta u_i^{n+1} + (1-\theta)u_i^n. \tag{18}$$

For our linear model problem, the artificial diffusion coefficients d_{ij} are independent of the solution but for nonlinear conservation laws they must be updated along with the operators K and L. The skew-symmetric fluxes f_{ij} represent the difference between the high-order scheme and the low-order one. Clearly, it is desirable to use the former as long as the imposed physical and/or mathematical constraints are satisfied. Otherwise, some artificial diffusion must be retained, i.e., the raw antidiffusive flux needs to be limited:

$$f_{ij}^* := \alpha_{ij} f_{ij}, \qquad \text{where} \quad 0 \leq \alpha_{ij} \leq 1. \tag{19}$$

A node-oriented limiting strategy which builds on the algebraic FCT and TVD schemes proposed previously [14],[15],[16] will be presented in the next section.

If implicit time-stepping ($0 < \theta \leq 1$) is employed, the nonlinear algebraic system at hand must be solved iteratively, e.g., by the defect correction scheme

$$u^{(m+1)} = u^{(m)} + [A(u^{(m)})]^{-1} r^{(m)}, \qquad m = 0, 1, 2, \ldots \tag{20}$$

where $r^{(m)}$ is the residual vector which includes the sum of limited antidiffusive fluxes

$$r^{(m)} = [M_L + (1-\theta)\Delta t L]u^n - [M_L - \theta \Delta t L]u^{(m)} + \Delta t F^*(u^{(m)}, u^n), \tag{21}$$

whereas $A(u^{(m)})$ is a suitably chosen 'preconditioner'. The typical choices are

$$A := M_L \tag{22}$$

(only suitable for very small time steps) and the low-order operator [14],[15]

$$A := M_L - \theta \Delta t L \tag{23}$$

which was designed to be an M-matrix. Alternatively, algebraic flux/defect correction schemes may be preconditioned by the nonlinear 'LED' operator

$$A(u^{(m)}) := M_L - \theta \Delta t L^*(u^{(m)}) \tag{24}$$

such that $L^*(u)u = Lu + F^*$ and $l^*_{ij} \geq 0,\ \forall j \neq i$. The existence of $L^*(u)$ is guaranteed by the flux limiter [16]. This kind of preconditioning renders all intermediate solutions $u^{(m)}$ positivity-preserving [11] but convergence is a prerequisite for mass conservation.

In a practical implementation, the 'inversion' of A is performed by an iterative method for solving the linear subproblem

$$A \Delta u^{(m+1)} = r^{(m)}, \qquad m = 0, 1, 2, \ldots \tag{25}$$

After a certain number of inner iterations, the solution increment $\Delta u^{(m+1)}$ is applied to the last iterate, whereby u^n provides a reasonable initial guess

$$u^{(m+1)} = u^{(m)} + \Delta u^{(m+1)}, \qquad u^{(0)} = u^n. \tag{26}$$

The iteration process is terminated when a certain norm of the defect $r^{(m)}$ or that of the relative changes $\Delta u^{(m+1)}$ becomes small enough. Explicit and/or implicit underrelaxation techniques may be invoked to secure the convergence of outer iterations [8].

5 Algebraic flux correction

The design philosophy of modern high-resolution schemes as presented by Zalesak [30] involves three main components which can be chosen and optimized individually:

1. an approximation to which they reduce in regions where the solution is smooth;
2. an approximation to which they reduce in the vicinity of shocks and steep fronts;
3. a mechanism for blending the above approximations at each node and time step so as to satisfy the imposed physical or mathematical criteria.

In the preceding three sections, we specified the first two components and showed how to combine them within an iterative defect correction scheme. Now we can proceed to the design of flux limiters to be used for the computation of the correction factors α_{ij} in (19). To this end, let us adopt a node-oriented limiting strategy which can be traced back to the flux-corrected transport (FCT) methodology [19],[28].

The limiting techniques to be considered are based on the following algorithm:

1. Compute the sums of positive/negative antidiffusive fluxes into each node.
2. Select *nodal correction factors* so as to satisfy the algebraic constraints.
3. Check the sign of the antidiffusive fluxes and limit them edge-by-edge.

Unlike many other algorithms, flux limiters of this form are fully multidimensional because they control the net antidiffusive flux / solution increment rather than the slope ratio for a local three-point stencil or a similar smoothness indicator [16]. Below we discuss different options for the choice and enforcement of appropriate upper/lower bounds.

5.1 Upwind-biased flux limiting

As demonstrated by Zalesak [29] for the one-dimensional advection equation $u_t + vu_x = 0$, where the velocity v is assumed to be positive, a family of upwind-biased flux limiters can be derived by imposing the TVD constraint on a suitable 'target flux' of the form

$$f_{ij} = \phi_{ij} d_{ij}(u_i - u_j), \tag{27}$$

where d_{ij} is an artificial diffusion coefficient. Typically, the Lax-Wendroff or central difference method serves as the high-order algorithm, while 'upwind' represents the monotone low-order one. The limited antidiffusive flux for a classical TVD scheme is given by

$$f_{ij}^* := \max\{0, \min\{2, \phi_{ij}, 2r_i\}\} d_{ij}(u_i - u_j) = \alpha_{ij} f_{ij}. \tag{28}$$

Importantly, the slope ratio $r_i = (u_i - u_k)/(u_j - u_i)$ is evaluated at the upwind node i.

Of course, the bounds imposed on f_{ij} are not optimal since the left boundary of the TVD region depends on the Courant number [10],[29]. However, ignoring this dependence in favor of the simple constraint $\alpha_{ij}\phi_{ij} \leq 2r_i$ (regardless of the time step) makes TVD-like limiters remarkably efficient and, moreover, directly applicable to stationary problems. To put it another way, instead of computing a sharp bound for a given time step (which is particularly expensive in multidimensions) one can use some reasonable fixed bounds and adjust the time step if this is necessary to satisfy a CFL-like condition.

The above interpretation reveals that the numerous 'limiter functions' proposed in the literature differ merely in the definition of the underlying target flux. Recall that any linear combination of the central difference / Lax-Wendroff method ($\phi_{ij} = 1$) and second-order upwind / Beam-Warming scheme ($\phi_{ij} = r_i$) yields a second-order accurate target flux. The most widely used TVD 'limiters' are as follows

minmod	$\phi_{ij} = \min\{1, r_i\}$,
Van Leer	$\phi_{ij} = 2r_i/(1 + r_i)$,
MC	$\phi_{ij} = (1 + r_i)/2$,
Koren	$\phi_{ij} = (2 + r_i)/3$,
superbee	$\phi_{ij} = \max\{1, r_i\}$.

The best accuracy attainable within Sweby's second-order TVD region is provided by Koren's limiter [12] which has been repeatedly reinvented under different names [1],[24]. Due to the fact that the leading terms in the modified equation cancel out, the resulting scheme is third-order accurate for sufficiently smooth data. We remark that all of the above approximations are only valid for a constant velocity v on a uniform 1D mesh.

Let us come back to the multidimensional continuity equation (1) and extend the above ideas to finite element discretizations on unstructured grids. In this case, the most natural choice of the target flux appears to be (17) or its lumped-mass counterpart which is appropriate for the treatment of steady or creeping flows:

$$f_{ij} = \phi_{ij} d'_{ij}(u_i - u_j), \qquad \text{where} \quad \phi_{ij} := d_{ij}/d'_{ij}. \tag{29}$$

Note that for a skew-symmetric transport operator $s_{ij} = 0$ and, consequently,

$$d_{ij} = d'_{ij}, \qquad \phi_{ij} = 1. \tag{30}$$

The family of high-resolution schemes proposed in [15],[16] is based on target fluxes constructed as for classical TVD methods (see above). To this end, the smoothness indicator r_i was redefined as the ratio of positive/negative edge contributions associated with positive/negative coefficients in the sum $\sum_{j\neq i} k'_{ij}(u_j - u_i) = f_i + g_i$, where

$$f_i = f_i^+ + f_i^-, \qquad f_i^\pm = \sum_{j\neq i} \min\{0, k'_{ij}\} \begin{matrix}\min\\ \max\end{matrix} \{0, u_j - u_i\}, \tag{31}$$

$$g_i = g_i^+ + g_i^-, \qquad g_i^\pm = \sum_{j\neq i} \max\{0, k'_{ij}\} \begin{matrix}\max\\ \min\end{matrix} \{0, u_j - u_i\}. \tag{32}$$

It is easy to verify that $r_i = g_i^\pm / f_i^\pm$ reduces to the usual slope ratio in the one-dimensional case [15],[16]. Constraining the target fluxes according to (28), one obtains a discretization which proves local extremum diminishing for any standard TVD limiter and returns a limited average of 'upwind' and 'downwind' edge contributions to each node. Although the results are typically quite good, the target fluxes for such an algorithm are inconsistent with the underlying Galerkin scheme and may fail to be second-order accurate on a nonuniform mesh. Furthermore, this sort of flux limiting requires mass lumping which is undesirable for strongly time-dependent problems. In the finite element framework, target fluxes of the form (17) or (29) are preferable because the high-order Galerkin approximation is recovered in regions where the solution is smooth enough.

The limited antidiffusive flux f_{ij}^* from node j into its upwind (in the sense of our orientation convention) neighbor i is given by relation (19). As proposed in [15],[16], positive and negative fluxes are treated separately, whereby the multipliers α_{ij} depend on the nodal correction factors $R_i^\pm$ (to be defined below) and on the magnitude of ϕ_{ij}

$$\alpha_{ij} = \begin{cases} \min\{R_i^+, 2/\phi_{ij}\}, & \text{if } f_{ij} > 0, \\ \min\{R_i^-, 2/\phi_{ij}\}, & \text{if } f_{ij} < 0, \end{cases} \qquad \alpha_{ji} := \alpha_{ij}. \tag{33}$$

In the trivial case $f_{ij} = 0$ no limiting is required. On the other hand, $|f_{ij}| > 0$ implies $|\phi_{ij}| > 0$ and $d'_{ij} > 0$ so that no division by zero takes place in the above relations.

Recall that the edges are oriented so that $l_{ij} = 0$ while $l_{ji} = 2d'_{ij} > 0$. Hence, the edge contribution to node j can be expressed as follows

$$k^*_{ji}(u_i - u_j) := 2d'_{ij}(u_i - u_j) - \alpha_{ij} f_{ij} \tag{34}$$

and due to (33) the off-diagonal coefficient in row j remains nonnegative:

$$k^*_{ji} = (2 - \min\{2, R^\pm_i \phi_{ij}\}) d'_{ij} \geq 0. \tag{35}$$

In order to make sure that the edge contribution to node i does not pose any hazard to positivity either, the sum of edge contributions from all downwind neighbors $j \neq i$ needs to be limited so as to enforce the corresponding upper/lower bounds. By definition,

$$R^\pm_i \leq 1 \quad \Rightarrow \quad \alpha_{ij} \leq \min\{1, 2/\phi_{ij}\}. \tag{36}$$

It follows that the 'downwind' antidiffusion into node i is bounded by

$$P^\pm_i = \sum_{j \neq i} \min\left\{1, \frac{\phi_{ij}}{2}\right\} l_{ji} \begin{matrix}\max\\ \min\end{matrix} \{0, u_i - u_j\} \tag{37}$$

which reduces to the sum $f^\pm_i$ in the special case of target fluxes given by (29)–(30).

In addition, the equivalent algebraic system (7) is supposed to satisfy the positivity constraint, at least for sufficiently small time steps or in the steady-state limit $u^{n+1} = u^n$. Therefore, the nodal correction factors are sought in the form

$$R^\pm_i = \min\{1, Q^\pm_i / P^\pm_i\}, \tag{38}$$

where the auxiliary quantities $Q^\pm_i$ admit the following representation

$$Q^\pm_i = \sum_{j \neq i} q^n_{ij} \begin{matrix}\max\\ \min\end{matrix} \{0, u^n_j - u^n_i\} + \sum_{j \neq i} q^{n+1}_{ij} \begin{matrix}\max\\ \min\end{matrix} \{0, u^{n+1}_j - u^{n+1}_i\}, \tag{39}$$

$$q^n_{ij} \geq 0, \quad q^{n+1}_{ij} \geq 0, \qquad \forall j \neq i. \tag{40}$$

Specifically, the upper/lower bounds for our algebraic TVD schemes read [15]

$$Q^\pm_i = \sum_{j \neq i} l_{ij} \begin{matrix}\max\\ \min\end{matrix} \{0, u_j - u_i\} = 2g^\pm_i, \tag{41}$$

where $l_{ij} = \max\{0, 2k'_{ij}\}$ are the coefficients of the low-order operator. The choice of $Q^\pm_i$ for finite element discretizations with a consistent mass matrix will be addressed below.

Let us summarize what we have said so far and piece together the revised algorithm for an upwind-biased flux correction of TVD type:

1. For each pair of neighboring nodes i and j, adopt the upwind-downwind edge orientation (!!!) and represent the target flux f_{ij} in terms of ϕ_{ij} such that

$$f_{ij} = \phi_{ij} d'_{ij}(u_i - u_j). \tag{42}$$

2. Prelimit f_{ij} and add its contribution to the sums $P_i^\pm$ initialized by zero

$$f_{ij} := \min\{1, 2/\phi_{ij}\} f_{ij}, \qquad P_i^\pm := P_i^\pm + \begin{matrix}\max\\ \min\end{matrix} \{0, f_{ij}\}. \tag{43}$$

3. Update the upper/lower bounds $Q_j^\mp$ initialized by zero, for instance

$$g_{ij} := 2d'_{ij}(u_i - u_j), \qquad Q_j^\mp := Q_j^\mp + \begin{matrix}\max\\ \min\end{matrix} \{0, g_{ij}\}. \tag{44}$$

4. Calculate the nodal correction factors and apply them edge-by-edge

$$f_{ij}^* := \begin{cases} R_i^+ f_{ij}, & \text{if } f_{ij} > 0, \\ R_i^- f_{ij}, & \text{if } f_{ij} < 0, \end{cases} \qquad R_i^\pm = \min\{1, Q_i^\pm / P_i^\pm\}. \tag{45}$$

5. Insert the limited antidiffusive fluxes f_{ij}^* into the defect vector (21)

$$r_i := r_i + \Delta t f_{ij}^*, \qquad r_j := r_j - \Delta t f_{ij}^*. \tag{46}$$

Remarkably, all the necessary information is extracted from the original matrix K and there is no need to know the coordinates of nodes or any other geometric details.

5.2 Symmetric flux limiting

For genuinely time-dependent problems, mass lumping degrades the phase accuracy of finite element schemes and deprives them of a significant advantage in comparison to finite difference and finite volume methods. Berzins [2],[3] recognized the need for including the consistent mass matrix in a positivity-preserving fashion and presented some ideas as to how this can be accomplished. As of this writing, no truly multidimensional extension of his methodology seems to be available, so we need to look for another way to embed the consistent mass matrix into algebraic flux correction schemes.

In fact, our revised FEM-TVD algorithm (42)-(46) is applicable to target fluxes of the form (17). However, the upper/lower bounds may need to be redefined as explained below and the mass matrix contribution may be large enough to render the upwind-biased limiting strategy impractical. As an alternative, we introduce a symmetric flux limiter which was largely inspired by the consistent-mass FEM-FCT algorithm [19],[20]. Let us start with a 'stand-alone' limiter for the mass antidiffusion $(M_L - M_C)\dot{u}$ such that

$$f_{ij} = m_{ij}(\dot{u}_i - \dot{u}_j) \tag{47}$$

and address the treatment of f_{ij} given by (17) with $d_{ij} \neq 0$ in the next subsection.

The first step is to specify suitable upper/lower bounds $Q_i^\pm$ to be imposed on the sum of raw antidiffusive fluxes $P_i^\pm$. Unlike those defined in (41), they should be applicable even in the case of a pure L_2-projection ($K = L = 0$). Let the contribution of the mass matrix to the right-hand side of the algebraic system (7) be represented in the form

$$b_i = m_i u_i^n + \Delta t \sum_{j \neq i} \alpha_{ij} f_{ij} = (m_i - c_i) u_i^n + c_i u_k^n, \tag{48}$$

where u_k^n is a local extremum (minimum or maximum over the set of nodes j such that $m_{ij} \neq 0$) and the coefficient c_i is defined by (cf. [13],[14])

$$c_i = \Delta t \, \frac{\sum_{j\neq i} \alpha_{ij} f_{ij}}{u_k^n - u_i^n}, \qquad u_k^n = \begin{cases} u_i^{\max} & \text{if } \sum_{j\neq i} \alpha_{ij} f_{ij} > 0, \\ u_i^{\min} & \text{if } \sum_{j\neq i} \alpha_{ij} f_{ij} < 0. \end{cases} \tag{49}$$

By construction, $c_i \geq 0$ and if there are no other contributions to the right-hand side, the positivity criterion is satisfied for $c_i \leq m_i$. In the presence of convective and diffusive terms, such a sharp estimate is also feasible [10] but computationally expensive. Therefore, it is worthwhile to relax the above condition so as to accommodate the contribution of the low-order transport operator and some 'convective' antidiffusion in what follows.

Recall that the target fluxes (47) correspond to a decomposition of the term

$$(M_L - M_C)\dot{u} = \frac{1}{\Delta t}(M_L - M_C)u^{n+1} + \frac{1}{\Delta t}(M_C - M_L)u^n. \tag{50}$$

The implicit part violates the M-matrix property in the left-hand side of (7) and, thus, is truly antidiffusive. At the same time, the off-diagonal coefficients of the explicit part are nonnegative and it turns out to be strongly *diffusive*. In fact, mass diffusion of this form has frequently been used for construction of 'monotone' low-order schemes to be combined with the underlying high-order ones in the finite element context [6],[19],[22],[23]. The maximum amount of artificial diffusion introduced thereby can be estimated by

$$(m_i - m_{ii})(u_i^{\min} - u_i^n) \leq \sum_{j\neq i} m_{ij}(u_j^n - u_i^n) \leq (m_i - m_{ii})(u_i^{\max} - u_i^n), \tag{51}$$

since $m_i = \sum_j m_{ij}$. These considerations have led us to require that the coefficient $m_i - c_i$ in (48) be bounded from below by the diagonal entry of the consistent mass matrix m_{ii}. That is, the diagonal coefficient for the L_2-projection with built-in mass antidiffusion should be bounded by those for the consistent and lumped mass matrices. To this end, the auxiliary quantities $P_i^{\pm}$ and $Q_i^{\pm}$ are redefined as follows

$$P_i^{\pm} = \sum_{j\neq i} \begin{matrix}\max\\ \min\end{matrix} \{0, f_{ij}\}, \qquad Q_i^{\pm} = \frac{m_i - m_{ii}}{\Delta t}(u_k^n - u_i^n) \tag{52}$$

and the nodal correction factors $R_i^{\pm}$ given by (38) are applied to the raw antidiffusive fluxes edge-by-edge. Note that it no longer makes sense to distinguish between 'upwind' and 'downwind' nodes because the flow direction is immaterial. If the skew-symmetric part is missing ($K' = 0$), the antidiffusive flux produces two negative off-diagonal coefficients. Hence, the minimum of nodal correction factors should be taken

$$\alpha_{ij} = \begin{cases} \min\{R_i^+, R_j^-\} & \text{if } f_{ij} > 0, \\ \min\{R_i^-, R_j^+\} & \text{if } f_{ij} < 0, \end{cases} \qquad \alpha_{ji} = \alpha_{ij}. \tag{53}$$

This symmetric limiting strategy has proved its worth in two-step FCT algorithms, whereby the local extrema of a provisional (low-order) solution are used to determine the upper and lower bounds such that $c_i \leq m_i$ [14],[16],[19],[28]. The use of slack bounds (52) based on the inequality $m_{ii} \leq m_i - c_i$ eliminates the need for computing an intermediate solution and leads to a marked improvement of the convergence rates.

A practical implementation of the above algorithm involves the following steps:

1. Initialize the auxiliary arrays thus: $P_i^\pm \equiv 0,\ Q_i^\pm \equiv 0,\ R_i^\pm \equiv 1.$

2. For each pair of neighboring nodes i and j, evaluate f_{ij} and add its contribution to the sums of positive/negative antidiffusive fluxes for both nodes

$$P_i^\pm := P_i^\pm + \genfrac{}{}{0pt}{}{\max}{\min}\{0, f_{ij}\}, \qquad P_j^\pm := P_j^\pm + \genfrac{}{}{0pt}{}{\max}{\min}\{0, -f_{ij}\}. \tag{54}$$

3. Update the maximum/minimum admissible increments for both nodes

$$Q_i^\pm := \genfrac{}{}{0pt}{}{\max}{\min}\left\{Q_i^\pm, u_j^n - u_i^n\right\}, \qquad Q_j^\pm := \genfrac{}{}{0pt}{}{\max}{\min}\left\{Q_j^\pm, u_i^n - u_j^n\right\}. \tag{55}$$

4. In a loop over nodes, scale the increments $Q_i^\pm$ so as to ensure that $m_{ii} \le m_i - c_i$ and compute the corresponding nodal correction factors from (38)

$$Q_i^\pm := \frac{m_i - m_{ii}}{\Delta t} Q_i^\pm, \qquad R_i^\pm := \min\{1, Q_i^\pm / P_i^\pm\}. \tag{56}$$

5. Limit the raw antidiffusive fluxes f_{ij} using the minimum of $R_i^\pm$ and $R_j^\mp$

$$f_{ij}^* := \begin{cases} \min\{R_i^+, R_j^-\} f_{ij} & \text{if } f_{ij} > 0, \\ \min\{R_i^-, R_j^+\} f_{ij} & \text{if } f_{ij} < 0. \end{cases} \tag{57}$$

6. Insert limited antidiffusion into the right-hand side and/or the defect vector

$$b_i := b_i + \Delta t f_{ij}^*, \qquad b_j := b_j - \Delta t f_{ij}^*. \tag{58}$$

Note that the bounds $Q_i^\pm$ depend on the local extrema of the old solution u^n and need to be updated just once per time step. For f_{ij} given by (47), the nodal correction factors $R_i^\pm$ are independent of Δt, since both $Q_i^\pm$ and $P_i^\pm$ are inversely proportional to it.

5.3 Combined flux limiting

In light of the above, mass antidiffusion can be limited as if spatial differential operators were missing and vice versa. The symmetric limiting strategy (54)-(58) is appropriate for the former, while upwind-biased flux limiting of the form (42)-(46) lends itself to the treatment of the convective term. However, such an 'operator splitting' for the target flux (17) is undesirable because the independent limiting of its constituents (29) and (47) may produce an antidiffusive flux of greater magnitude than the original one. Indeed, the contribution of the consistent mass matrix and convective antidiffusion may have different signs. Our experience with flux correction of FCT type indicates that it is worthwhile to prelimit f_{ij} so as to prevent it from becoming diffusive and creating numerical artifacts [13],[16]. The corresponding coefficient ϕ_{ij}^T for the total flux (17) reads

$$\phi_{ij}^T = \max\{0, m_{ij}(\dot{u}_i - \dot{u}_j)/(u_i - u_j) + d_{ij}\}/d'_{ij}. \tag{59}$$

It remains to specify the upper/lower bounds and choose the algorithm for enforcing them. The above flux limiters can be combined in the following straightforward way:

1. Limit the target fluxes $f_{ij} := \phi_{ij}^T d'_{ij}(u_i - u_j)$ following the upwind-biased algorithm (42)-(46) with $P_i^\pm$ and $Q_i^\pm$ defined as in (37) and (41), respectively

$$f_{ij}^* := \min\{R_i^\pm, 2/\phi_{ij}^T\} f_{ij}. \tag{60}$$

2. Limit the rejected antidiffusion $\Delta f_{ij} = f_{ij} - f_{ij}^*$ in a symmetric fashion according to (54)-(58) with $P_i^\pm$ and $Q_i^\pm$ defined as in (52) to compute the correction

$$\Delta f_{ij}^* := \min\{R_i^\pm, R_j^\mp\} \Delta f_{ij}. \tag{61}$$

Alternatively, it is possible to invoke the upwind-biased flux limiter with $P_i^\pm$ given by (37) and $Q_i^\pm$ redefined as the sum of bounds for the two steps of the above algorithm

$$Q_i^\pm := \frac{m_i - m_{ii}}{\Delta t}(u_i^* - u_i^n) + \sum_{j \neq i} l_{ij} \begin{matrix} \max \\ \min \end{matrix} \{0, u_j - u_i\}. \tag{62}$$

This scenario is certainly cheaper than the use of symmetric 'postlimiting' but typically less accurate because of the restriction $\alpha_{ij} \leq \min\{1, 2/\phi_{ij}^T\}$ imposed by the positivity condition for the downwind node j. It is not unusual that $\phi_{ij}^T \gg 2$ if mass antidiffusion is strong enough, which means that a significant portion of the target flux cannot be recovered by the upwind-biased flux limiter alone. Likewise, symmetric flux limiting with $Q_i^\pm$ given by (62) is feasible but not as accurate as the two-step algorithm because the minimum of nodal correction factors needs to be taken in (53).

In either case, the effective upper/lower bounds for the net antidiffusive flux consist of a 'stationary' part (41) which is defined as in algebraic TVD schemes and a 'time-dependent' part (52) which may be dropped if mass lumping is in order ($m_{ij} = 0$, $\forall j \neq i$). This two-step approach to the definition of nodal constraints leads to an algorithm which combines the advantages of FCT- and TVD-like schemes:

- Due to (41), the use of large time steps for steady-state computations does not lead to a loss of accuracy, as the correction factors become largely independent of Δt.
- By virtue of (52), solutions to truly time-dependent problems become more accurate as Δt is refined, since a larger portion of the target flux may be retained.

Both constituents of $Q_i^\pm$ were constructed using heuristic arguments rather than the intrinsic 'CFL' condition which requires that the diagonal coefficient in the right-hand side of (7) be nonnegative for a given Δt. Such estimates would be expensive to obtain and sometimes overly restrictive, e.g., for stationary problems solved by time marching. Therefore, we deliberately relax them to make the algorithm more efficient, improve the convergence rates, and satisfy the discrete maximum principle in the steady-state limit.

Of course, there are many other ways to select and enforce the upper/lower bounds. Moderate improvements can be achieved – at a disproportionately high overhead cost – but our numerical experiments indicate that the accuracy of the underlying target flux rather than the choice of constraints and the type of flux limiter is decisive in many cases. Roughly speaking, it is not the limiter but the antidiffusive flux itself that still needs to be optimized. In the finite element context, the use of time-accurate Taylor-Galerkin methods (for transient problems) and/or high-order basis functions appears to be a promising way to improve the performance of algebraic flux correction schemes.

6 Numerical examples

In order to illustrate the ideas presented in this paper, we apply the new limiting strategy to equation (1) discretized in space by P_1/Q_1 finite elements. For a detailed numerical study of its FCT and TVD prototypes which covers an extension of the algebraic flux correction paradigm to nonlinear PDE systems (Euler equations, Navier-Stokes equations, $k-\varepsilon$ turbulence model), the interested reader is referred to [16],[17],[25].

6.1 Convection of a square wave

Let us start with a classical test problem which consists of solving the one-dimensional convection equation $u_t + vu_x = 0$ for discontinuous initial data depicted as dashed lines in Fig. 1. The dotted lines show the exact solution for $v = 1$ and $t = 0.5$ which is obtained by translation of the initial profile along the $x-$axis. The domain $(0, 1)$ is discretized by linear finite elements of equal length $\Delta x = 10^{-2}$. The discretization in time is performed by the second-order accurate Lax-Wendroff method. The time step $\Delta t = 10^{-3}$ used to compute the numerical solutions in Fig. 1 corresponds to a Courant number of 0.1. The behavior of standard TVD schemes for this simple test problem is well known. As usual, the most diffusive results are produced by the *minmod* limiter, while *superbee* performs best on such discontinuous solutions but tends to corrupt smooth profiles due to artificial steepening. Limiters like MC produce acceptable results in either case and are typically used by default. For the square wave problem, the MC limiter proves far superior to *minmod* but less accurate than *superbee*, see Fig. 1a-c.

The target flux given by $\phi_{ij} = 1$ corresponds to the finite difference Lax-Wendroff scheme which can be classified as a lumped-mass (LM) Taylor-Galerkin method of second order. As shown in Fig. 1d, the resulting solution is asymmetric, whereby the right flank of the square wave is reproduced much better than the left one. The latter is smeared as much as that for *minmod*, which is due to mass lumping. Adding the contribution of the consistent mass (CM) matrix yields a target flux with improved phase characteristics [5]. Limiting it as before in accordance with (28) is equivalent to (60) in our two-step approach to combined flux limiting. The numerical solution displayed in Fig. 1e resembles that produced by *superbee*. Note that the upper right corner of the square wave remains 'rounded' because the bounds (41) are too restrictive for transient problems. This can be rectified by resorting to symmetric postlimiting (61) which yields an equally crisp resolution of both flanks, see Fig. 1f. We conclude that the use of a consistent mass matrix is essential not only for the definition of the target flux but also for the estimation of upper/lower bounds in finite element schemes based on algebraic flux correction.

6.2 Convection of a semi-ellipse

Our second test problem is a slightly modified version of the one used in [21],[29],[30] to expose the 'terracing' phenomenon, an infamous byproduct of flux limiting. The linear convection equation is solved for continuous initial data given by the formula

$$u(x, 0) = \sqrt{1 - \left(\frac{x - 0.2}{0.15}\right)^2} \qquad \text{if} \quad |x - 0.2| \leq 0.15 \tag{63}$$

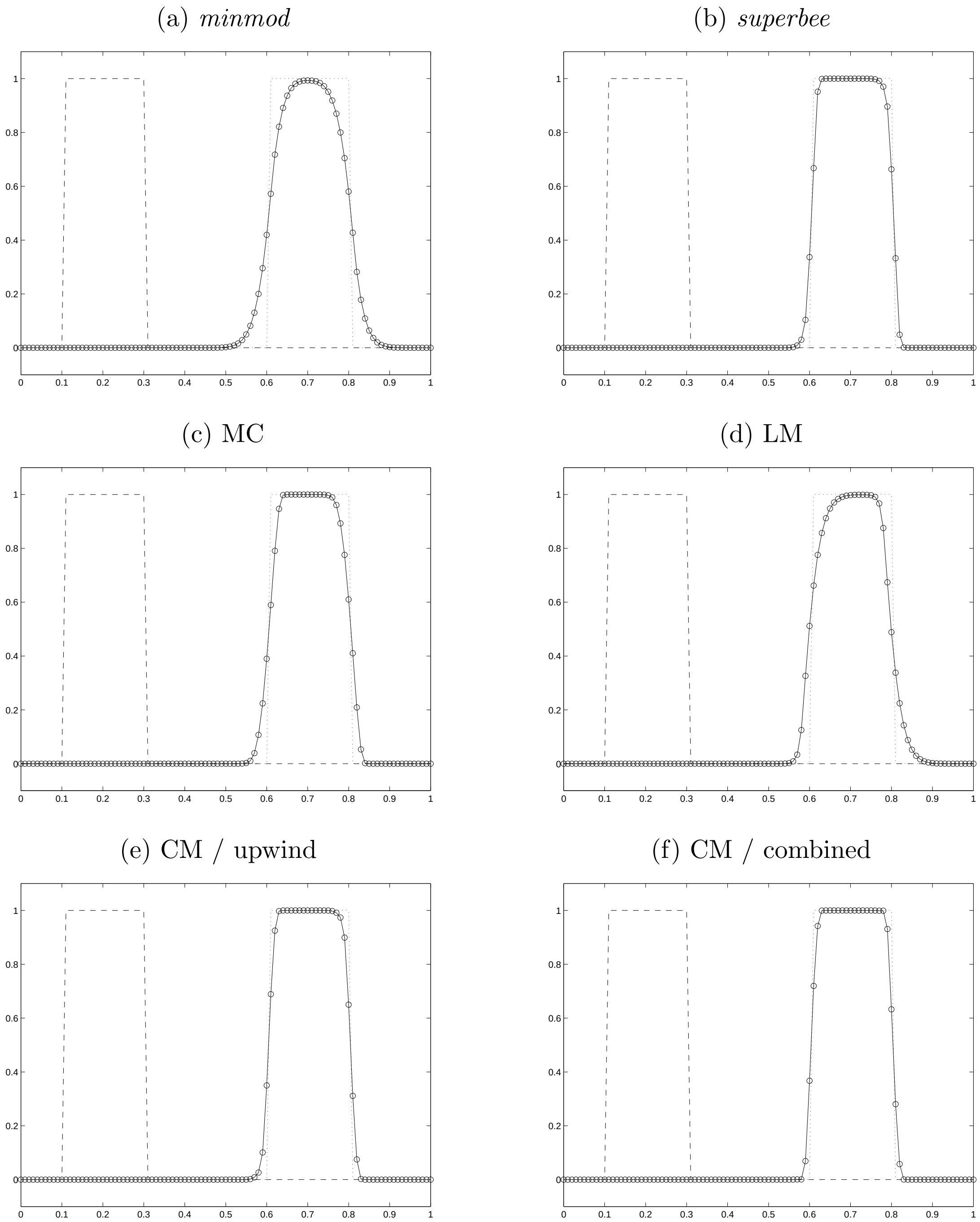

Figure 1. Convection of a square wave: numerical solutions at $t = 0.5$.

and $u(x, 0) = 0$ otherwise. All discretization parameters are the same as in the first example. The challenge of the second test consists in resolving the steep parts of the otherwise smooth profile without generating spurious kinks or plateaus. Such a nonphysical solution behavior, which is a common drawback of many modern high-resolution schemes, is referred to as terracing and can be interpreted as 'an integrated, nonlinear effect of residual phase errors' [21] or, loosely speaking, 'the ghosts of departed ripples' [4].

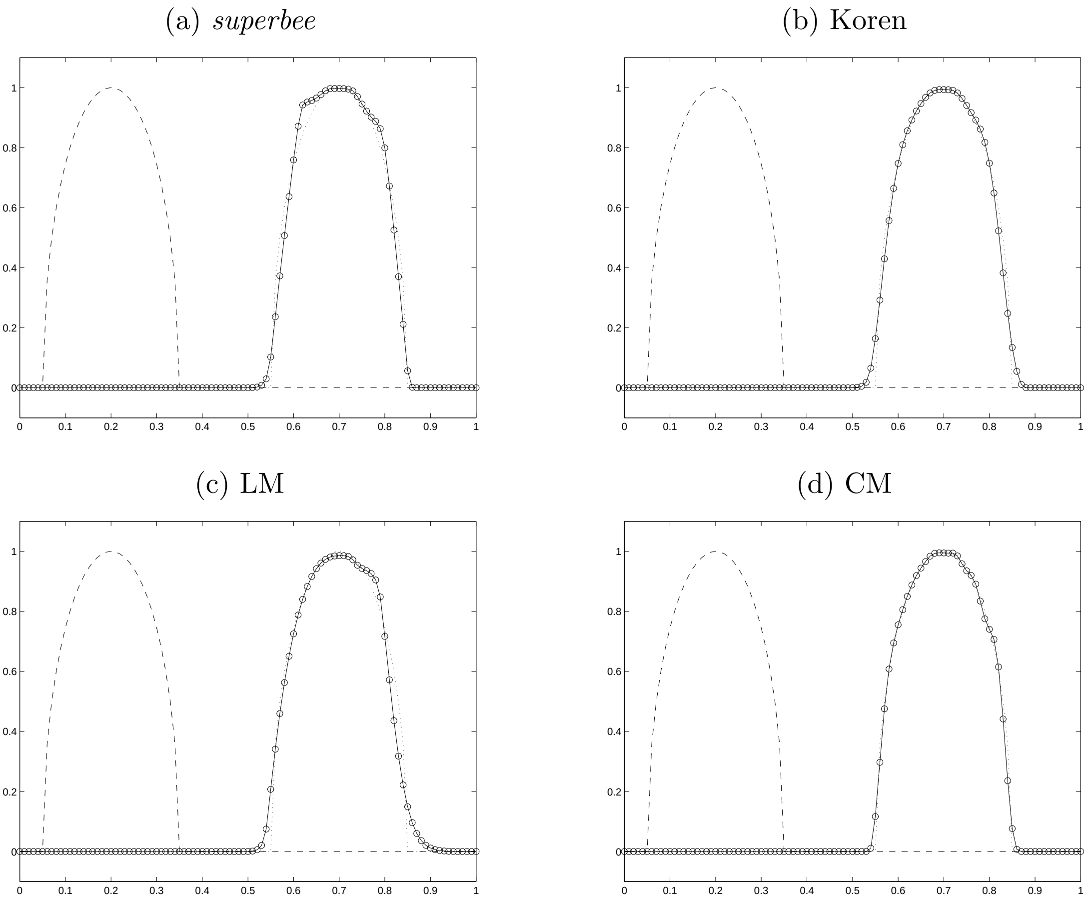

Figure 2. Convection of a semi-ellipse: numerical solutions at $t = 0.5$.

Terracing was first discovered in the FCT context but it is also typical of TVD limiters like *superbee*, see Fig. 2a. The best results for this benchmark problem are produced by Koren's limiter (Fig. 2b) which is based on a third-order accurate target flux. In the finite element framework, mass lumping tends to aggravate phase errors, which manifests itself in a pronounced terracing (Fig. 2c). The solution displayed in Fig. 2d illustrates the benefits of using the consistent mass matrix in conjunction with the two-step limiting strategy. The observed improvement in comparison to the lumped-mass version supports the conjecture that terracing can be cured to some extent by increasing the resolving power of the target flux so as to reduce the dispersive errors [29],[30]. Numerical experiments indicate that the small but still noticeable deviations from the exact shape at the right edge of the semi-ellipse in Fig. 2d are caused by the fluxes that prove insufficiently antidiffusive (more diffusive than *minmod*) in spite of the prelimiting performed in (17). Indeed, false diffusion cannot be detected by the flux limiter and should be filtered out beforehand.

6.3 Solid body rotation

Let us proceed to the two-dimensional benchmark problem proposed by LeVeque [18] which makes it possible to assess the ability of a high-resolution scheme to preserve both smooth and discontinuous profiles. To this end, a slotted cylinder, a sharp cone and a smooth hump are exposed to the nonuniform velocity field $\mathbf{v} = (0.5 - y, x - 0.5)$ and undergo a counterclockwise rotation about the center of the unit square $\Omega = (0,1)\times(0,1)$. Each solid body lies within a circle of radius $r_0 = 0.15$ centered at a point with Cartesian coordinates (x_0, y_0). In the rest of the domain, the solution is initialized by zero. The shapes of the three bodies as depicted in Fig. 3 can be expressed in terms of the normalized distance function for the respective reference point (x_0, y_0) thus:

$$r(x,y) = \frac{1}{r_0}\sqrt{(x-x_0)^2 + (y-y_0)^2}.$$

The center of the slotted cylinder is located at $(x_0, y_0) = (0.5, 0.75)$ and its geometry in the circular region $r(x,y) \leq 1$ is given by

$$u(x,y,0) = \begin{cases} 1 & \text{if } |x - x_0| \geq 0.025 \ \vee \ y \geq 0.85, \\ 0 & \text{otherwise.} \end{cases}$$

The corresponding analytical expression for the conical body reads

$$u(x,y,0) = 1 - r(x,y), \qquad (x_0, y_0) = (0.5, 0.25),$$

whereas the shape and location of the hump at $t = 0$ are as follows

$$u(x,y,0) = 0.25[1 + \cos(\pi \min\{r(x,y), 1\})], \quad (x_0, y_0) = (0.25, 0.5).$$

After one full revolution ($t = 2\pi$) the exact solution of the continuity equation (1) coincides with the initial data. The numerical solutions presented in Fig. 4-6 were computed on a uniform mesh of 128×128 bilinear finite elements using the second-order accurate Crank-Nicolson time-stepping ($\theta = 0.5$) with $\Delta t = 10^{-3}$. The consistent-mass (CM) algorithm (60)-(61) produces the most accurate results shown in Fig. 4. The cone and hump are reproduced very well and even the narrow bridge of the slotted cylinder is largely preserved. Not surprisingly, this solution is very similar to that computed by an FCT algorithm based on the same target flux [14]. In either case, the prelimiting of antidiffusive fluxes in (59) is essential. If it is not performed, the ridges of the cylinder are subject to spurious erosion which can be interpreted as a sort of terracing.

By contrast, the performance of standard TVD limiters for this time-dependent test problem leaves a lot to be desired. The strong antidiffusion inherent to *superbee* alleviates the diffusive effect of mass lumping and yields a fairly good resolution of the slotted cylinder (Fig. 5) but entails a pronounced flattening of the smooth peaks. The numerical solution produced by the 'default' MC limiter (Fig. 6) exhibits both a strong smearing of the slotted cylinder and a noticeable distortion of the cone and hump.

6.4 Convection in space-time

If the problem at hand is stationary, the time derivative vanishes and so does the contribution of the consistent mass matrix. Therefore, mass lumping is appropriate, i.e., the raw antidiffusive flux is given by (29) and symmetric postlimiting (61) can/should be omitted. Due to the fact that the upper/lower bounds for the upwind-biased part (60) are

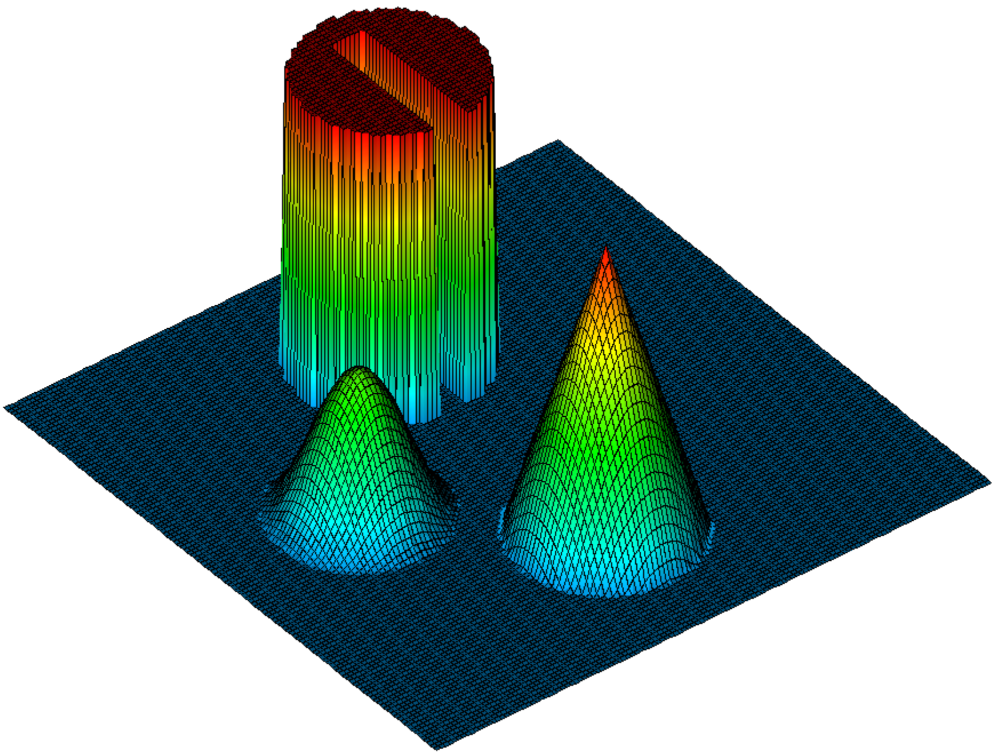

Figure 3. Solid body rotation: initial data / exact solution.

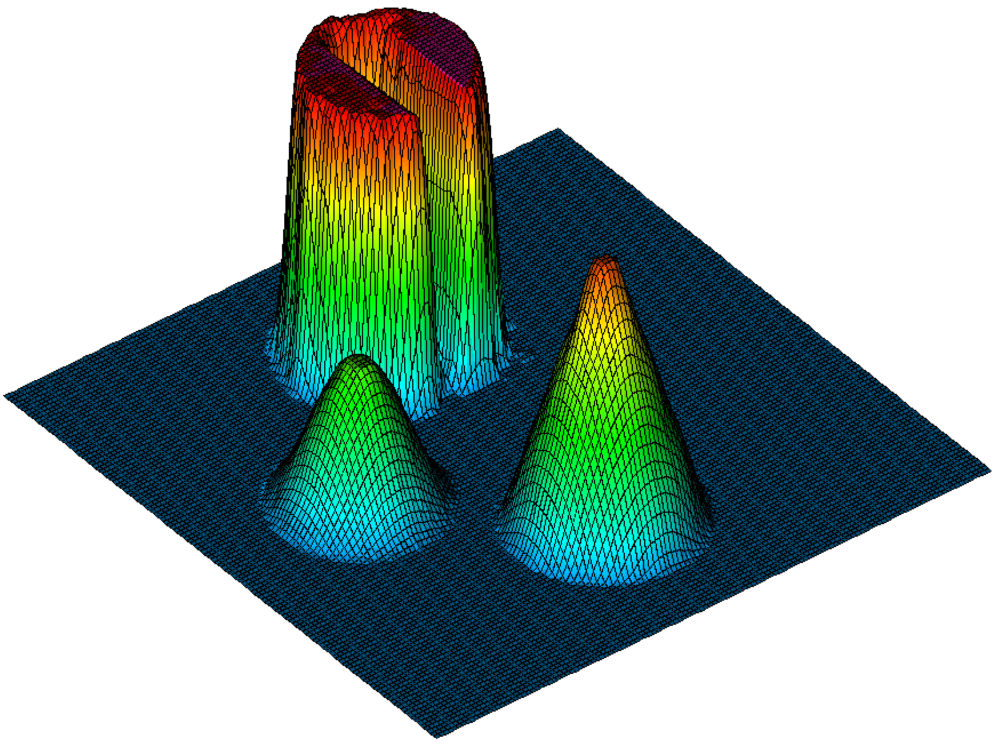

Figure 4. Solid body rotation: CM limiter, $t = 2\pi$.

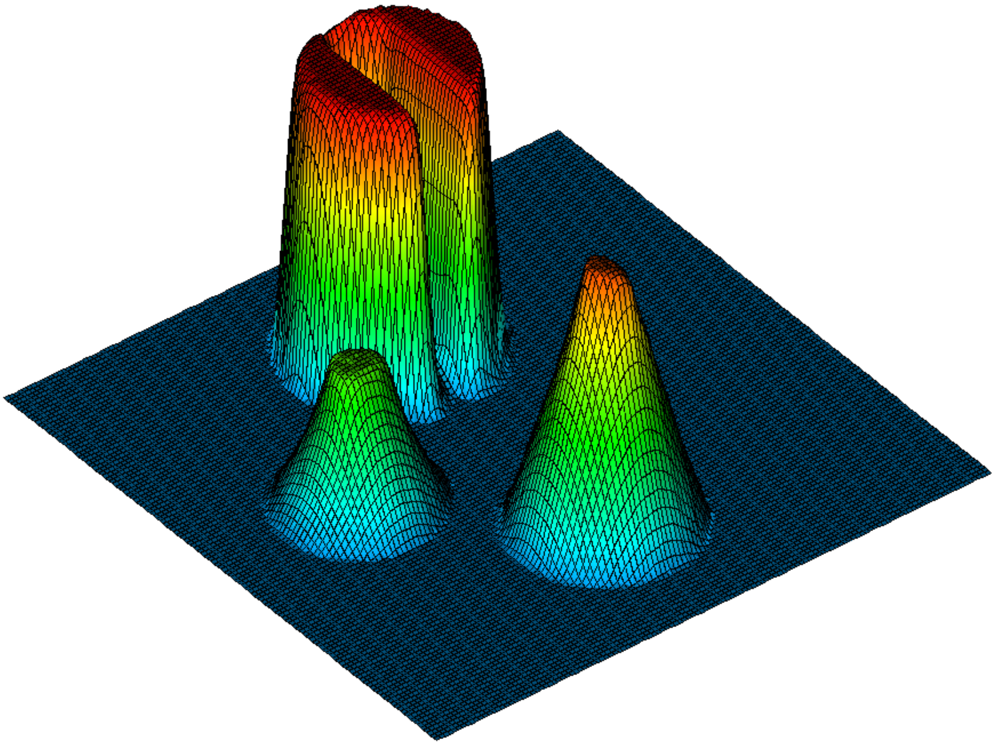

Figure 5. Solid body rotation: *superbee* limiter, $t = 2\pi$.

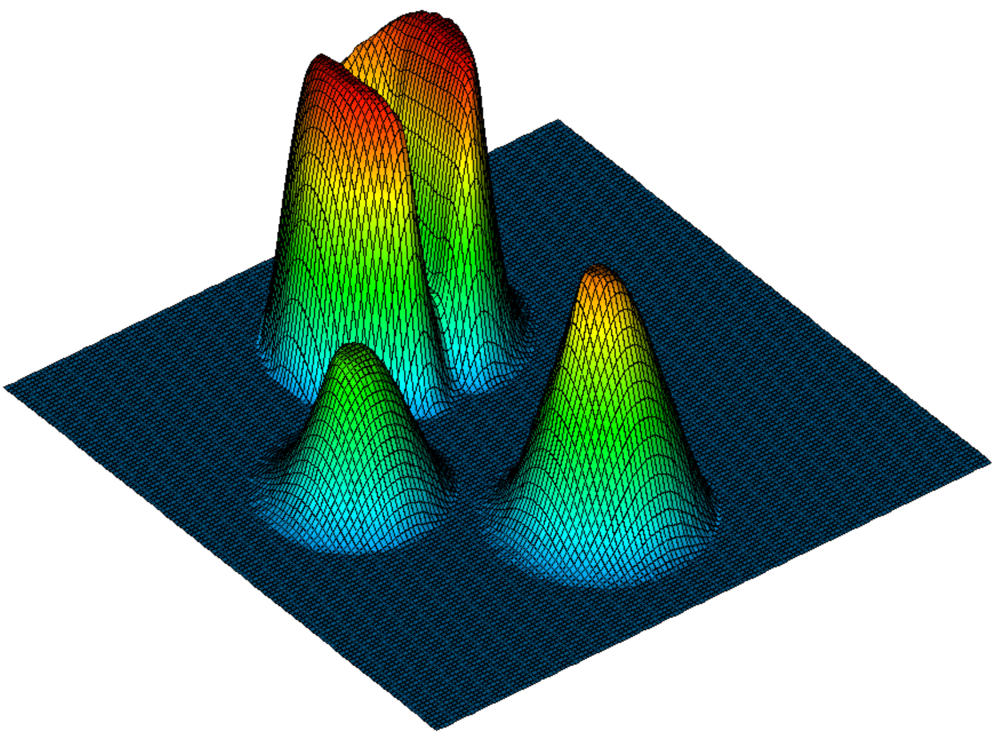

Figure 6. Solid body rotation: MC limiter, $t = 2\pi$.

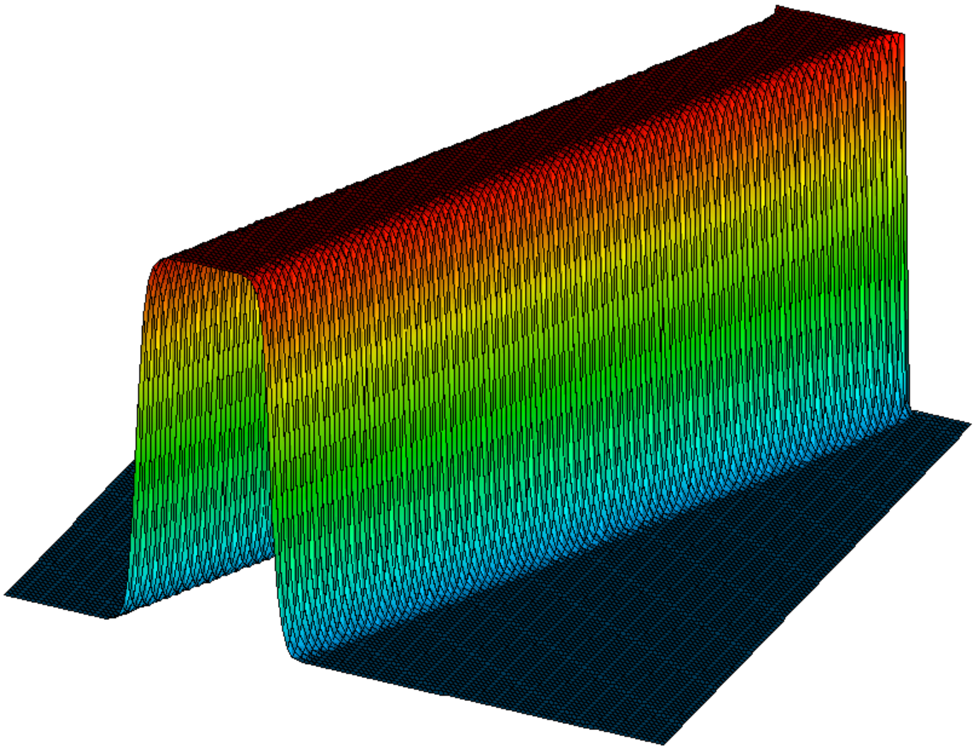

Figure 7. Convection in space-time: LM limiter.

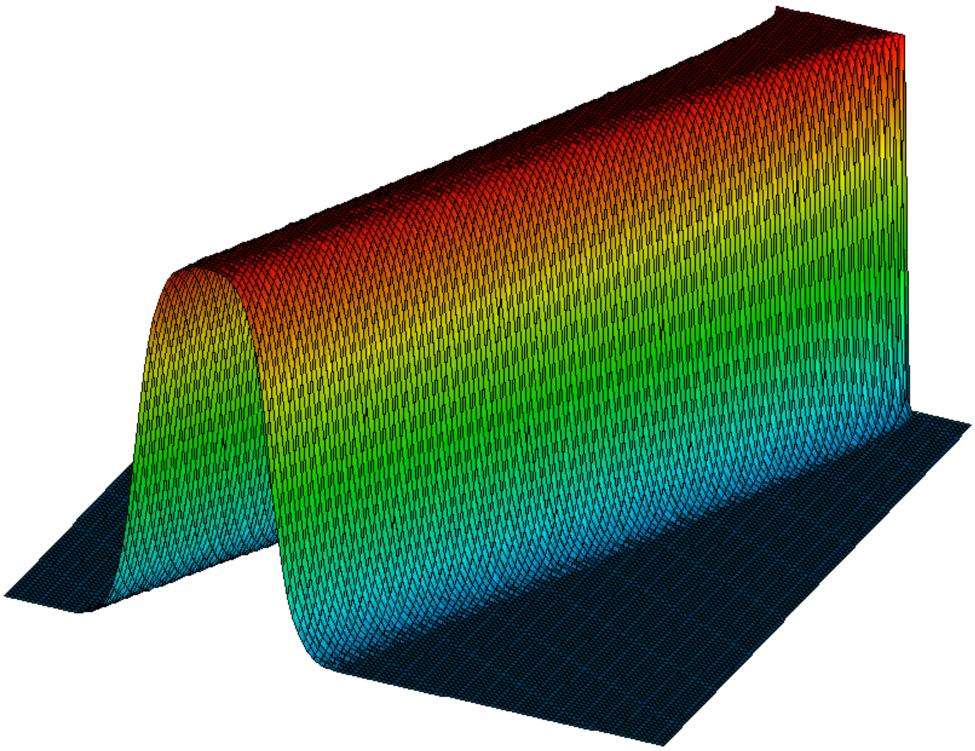

Figure 8. Convection in space-time: *minmod* limiter.

independent of the time step, it is possible to compute the steady-state solution directly or by means of pseudo-time-stepping based on the fully implicit backward Euler scheme ($\theta = 1$). In the latter case, the time step represents a variable underrelaxation parameter [8] which should be chosen as large as possible to reduce the computational cost. For an FCT-like limiter, whereby each solution update is required to be positivity-preserving, this would entail an irrecoverable loss of accuracy, since the nodal correction factors are inversely proportional to Δt. At the same time, our new algorithm is free of this drawback because it reduces to a TVD-like method for large time steps.

Let us return to the square wave test and reformulate the one-dimensional convection equation with $v = 0.5$ as a stationary problem of the form (1) with $\mathbf{v} = (0.5, 1)$. This corresponds to computing the solution for all time levels simultaneously instead of doing it step-by-step as usual [16]. The following initial/boundary conditions are imposed at the 'inlet' of the space-time domain $\Omega = (0, 1) \times (0, 1)$

$$u(0, t) = 0, \qquad u(x, 0) = \begin{cases} 1 & \text{if } |x - 0.2| \leq 0.1, \\ 0 & \text{otherwise.} \end{cases}$$

The numerical results obtained using algebraic flux correction based on the lumped-mass (LM) Galerkin flux and the standard *minmod* limiter are presented in Fig. 7 and Fig. 8, respectively. Both solutions were marched to the steady state by the backward Euler method, whereby the time step $\Delta t = 1.0$ was intentionally chosen to be very large. The discontinuous initial profile is shown in the background, while the solution at time $t = 1$ appears in the front. This example demonstrates that even in the stationary case the new algorithm is much better than *minmod*, the only standard TVD limiter which is consistent with the underlying finite element scheme.

7 Conclusions

In this paper, we focused on the design of flux limiters for finite element discretizations with a consistent mass matrix. Algebraic constraints were imposed node-by-node so as to control the contribution of negative off-diagonal coefficients in the corresponding rows of the discrete transport operator. Upper/lower bounds for the sum of positive/negative antidiffusive fluxes were designed so as to satisfy the M-matrix property for an equivalent algebraic system. A combination of the bounds derived separately for the special cases of consistent-mass L_2-projection and lumped-mass Galerkin approximation was found to strike the balance between accuracy and efficiency. The choice of high-order target fluxes was addressed and a fully multidimensional limiting strategy was presented. The new algorithm which combines the advantages of algebraic FCT and TVD schemes [14],[15] is capable of producing excellent results for stationary and time-dependent problems alike. In the latter case, the phase accuracy can be improved in the framework of Taylor-Galerkin methods [5]. Furthermore, high-order finite elements / bubble functions lend themselves to the design of target fluxes. These outstanding issues constitute an interesting direction for further research. An extension of the proposed methodology to the Euler and Navier-Stokes equations of fluid dynamics can be readily performed as explained in [17],[25].

References

[1] M. Arora and P. L. Roe, A well-behaved TVD limiter for high-resolution calculations of unsteady flow. *J. Comput. Phys.* **132** (1997) 3-11.

[2] M. Berzins, Modified mass matrices and positivity preservation for hyperbolic and parabolic PDEs. *Commun. Numer. Methods Engrg.* **17** (2001) no. 9, 659-666.

[3] M. Berzins, Variable-order finite elements and positivity preservation for hyperbolic PDEs. *Appl. Numer. Math.* **48** (2004) no. 3-4, 271-292.

[4] D. L. Book, The conception, gestation, birth, and infancy of FCT. In: D. Kuzmin, R. Löhner and S. Turek (eds.) *Flux-Corrected Transport: Principles, Algorithms, and Applications.* Springer, 2005, 5-28.

[5] J. Donea, L. Quartapelle and V. Selmin, An analysis of time discretization in the finite element solution of hyperbolic problems. *J. Comput. Phys.* **70** (1987) 463–499.

[6] J. Donea, V. Selmin and L. Quartapelle, Recent developments of the Taylor-Galerkin method for the numerical solution of hyperbolic problems. *Numerical methods for fluid dynamics III*, Oxford, 171-185 (1988).

[7] J. Donea, B. Roig and A. Huerta, High-order accurate time-stepping schemes for convection-diffusion problems. *Comput. Methods Appl. Mech. Eng.* **182** (2000) no. 3-4, 249-275.

[8] J. H. Ferziger and M. Peric, *Computational Methods for Fluid Dynamics.* Springer, 1996.

[9] C. A. J. Fletcher, The group finite element formulation. *Comput. Methods Appl. Mech. Engrg.* **37** (1983) 225-243.

[10] K. Hain, The partial donor cell method. *J. Comput. Phys.* **73** (1987) 131-147.

[11] T. Jongen and Y.P. Marx, Design of an unconditionally stable, positive scheme for the $K-\varepsilon$ and two-layer turbulence models. *Comput. Fluids* **26** (1997) no. 5, 469-487.

[12] B. Koren, A robust upwind discretization method for advection, diffusion and source terms. In: C. B. Vreugdenhil *et al.* (eds.), *Numerical methods for advection - diffusion problems.* Braunschweig: Vieweg. *Notes Numer. Fluid Mech.* **45** (1993) 117-138.

[13] D. Kuzmin and S. Turek, Flux correction tools for finite elements. *J. Comput. Phys.* **175** (2002) 525-558.

[14] D. Kuzmin, M. Möller and S. Turek, High-resolution FEM-FCT schemes for multidimensional conservation laws. *Computer Meth. Appl. Mech. Engrg.* **193** (2004) 4915-4946.

[15] D. Kuzmin and S. Turek, High-resolution FEM-TVD schemes based on a fully multidimensional flux limiter. *J. Comput. Phys.* **198** (2004) 131-158.

[16] D. Kuzmin and M. Möller, Algebraic flux correction I. Scalar conservation laws. In: D. Kuzmin, R. Löhner and S. Turek (eds.) *Flux-Corrected Transport: Principles, Algorithms, and Applications*. Springer, 2005, 155-206.

[17] D. Kuzmin and M. Möller, Algebraic flux correction II. Compressible Euler equations. In: D. Kuzmin, R. Löhner and S. Turek (eds.) *Flux-Corrected Transport: Principles, Algorithms, and Applications*. Springer, 2005, 207-250.

[18] R. J. LeVeque, High-resolution conservative algorithms for advection in incompressible flow. *Siam J. Numer. Anal.* **33** (1996) 627–665.

[19] R. Löhner, K. Morgan, J. Peraire and M. Vahdati, Finite element flux-corrected transport (FEM-FCT) for the Euler and Navier-Stokes equations. *Int. J. Numer. Meth. Fluids* **7** (1987) 1093–1109.

[20] R. Löhner, *Applied CFD Techniques: An Introduction Based on Finite Element Methods*. Wiley, 2001.

[21] E. S. Oran and J. P. Boris, *Numerical Simulation of Reactive Flow*. 2nd edition, Cambridge University Press, 2001.

[22] V. Selmin, Finite element solution of hyperbolic equations. I. One-dimensional case. *INRIA Research Report* **655** (1987).

[23] V. Selmin, Finite element solution of hyperbolic equations. II. Two-dimensional case. *INRIA Research Report* **708** (1987).

[24] A. Sokolichin, *Mathematische Modellbildung und numerische Simulation von Gas-Flüssigkeits-Blasenströmungen*. Habilitation thesis, University of Stuttgart, 2004.

[25] S. Turek and D. Kuzmin, Algebraic flux correction III. Incompressible flow problems. In: D. Kuzmin, R. Löhner and S. Turek (eds.) *Flux-Corrected Transport: Principles, Algorithms, and Applications*. Springer, 2005, 251-296.

[26] R. W. C. P. Verstappen and A. E. P. Veldman, Preserving symmetry in convection-diffusion schemes. In: D. Drikakis and J. Geurts (eds.) *Turbulent flow computation*, Fluid Mechanics and its Applications **6**. Dordrecht: Kluwer, 2002.

[27] R. W. C. P. Verstappen and A. E. P. Veldman, Symmetry-preserving discretization of turbulent flow. *J. Comput. Phys.* **187** (2003) 343-368.

[28] S. T. Zalesak, Fully multidimensional flux-corrected transport algorithms for fluids. *J. Comput. Phys.* **31** (1979) 335–362.

[29] S. T. Zalesak, A preliminary comparison of modern shock-capturing schemes: linear advection. In: R. Vichnevetsky and R. Stepleman (eds.) *Advances in Computer Methods for PDEs*. Publ. IMACS, 1987, 15-22.

[30] S. T. Zalesak, The design of Flux-Corrected Transport (FCT) algorithms for structured grids. In: D. Kuzmin, R. Löhner and S. Turek (eds.) *Flux-Corrected Transport: Principles, Algorithms, and Applications*. Springer, 2005, 29-78.